Sreyas International Journal of Scientists and Technocrats, Vol. 2 (4) 2018, pp. 38 -46

ORGINAL ARTICLE

Residual Stresses and Distortions of Welding Process: Simulation of Martensitic Steels

*** D V Paleshwar[1], Suresh Akella[1], T. Mohan Das[2], ACS Kumar[3].**

[1] Department of Mechanical Engineering, Sreyas Institute of Engineering and Technology, Hyderabad, India.

[2]Retired Scientist F, DMRL, [3] Professor , J.B. Institute of Engineering & Technology, Hyderabad, India.

Received- 2 Feb 2018, Revised- 14 March 2018, Accepted- 21 March 2018, Published- 01 Apr 2018

ABSTRACT

Martensite steels are required for high temperature applications where hardness is required. In this study, four grades of Martensite steels are compared in a 1D model simulation of welding, where a sequential thermal and structural analysis is done. The welding heat flux with thermal boundary conditions gives the temperature distribution. The structural boundary conditions along with lateral welding process are taken as a parameter variation direction, applying symmetric conditions. Thermal Load Affect is carried out for structural variations of distortion and stress as a decoupled system. All calculations are done in MS Excel. The **t**hermal stresses are about 30 times more than the elastic stresses causing the residual stress affect

Keywords: Martensite Steel, Weld Finite Element, Thermo mechanical affects, distortion, and residual stresses..

1. INTRODUCTION

The basic objective of this study is to provide a 1D Finite element model for the welding process. Many books have dealt with the subject of heat transfer models [1], [2] and [3] Welding is a thermo metallurgical and structural problem, a coupled formulation is preferred but it became complicated for analysis. A decoupled or sequential simulation is implemented in this study using a 1D finite element in the lateral direction to the weld direction. The heat of weld is evaluated with thermal load and boundary conditions of the temperature distribution. The temperature distribution is taken as a load and sequentially applied to the structural stiffness element and structural boundary conditions again evaluated as elimination from the heat transfer analysis obtained by the temperature distribution due to the heat of welding which is modeled using Load Vector. The 1D model also uses the symmetry of thermal load and material in the base materials joined by lap welding process. The variation is assumed only in the lateral direction and it is assumed to be same along the depth and the thickness resulting in the simple 1D model. Welding in lap joint is done by providing temperature above the 1460^{o}C at the weld fusion zone. The distribution is seen as a temperature nodal output. Linear shape functions are used to obtain, conduction, convection and load vectors. In further study the temperature output is used in obtaining structural distortion and residual stresses.

The Wear resistance properties of Martenstic steels [9] for high stiffness to mass ratio, the coefficient of thermal expansion for such material is given in terms of atomic percentage of carbon in Marten site.

2. RELATED THERMO-STRUCTURAL MODELS

The structural load on a material gives a flexural distortion and stresses which disappear once the load is removed. But thermal load causes residual strain, distortion and stresses which remains same in the system after the heat of thermal distribution is removed as it gets absorbed in the material as per the coefficient of thermal expansion. In the following part of the report modeling of the thermal load and resulting displacements and stresses are discussed.

*Corresponding author. Tel.: +919441119513
Email address: paleshwar.d@sreyas.ac.in (D V Paleshwar)
Double blind peer review under responsibility of SERAYAS Publications
https://dx.doi.org/10.24951/sreyasijst.org/2018041004

3. FINITE ELEMENT SIMULATION MODELING

3.1 Temperature Effects

In an isotropic linearly elastic material, a heat load causes temperature distribution. The difference in temperature is the cause of heat flow. The thermal stress problem is due to a distribution of change in temperature, $\Delta T(x)$, which causes a change in length and the strain is due to the change in temperature and it can be treated as an initial strain,ϵ_0, given by Eq. (1)

$$\epsilon_0 = \alpha \Delta T \qquad (1)$$

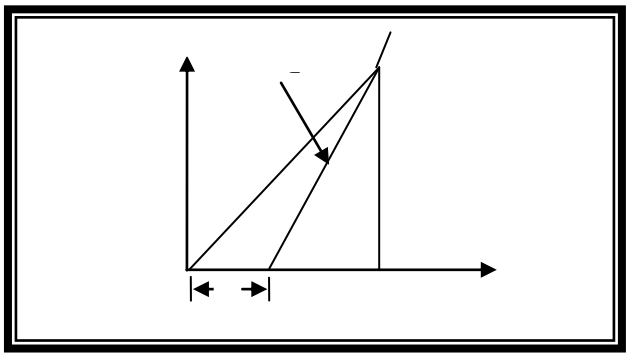

Figure 1. Stress – Strain in the presence of an Initial Thermal Strain.

Where α is the coefficient of thermal expansion. it is to be mentioned that a positive ΔT implies a rise in temperature. The stress – strain law in the presence of ϵ_0 is shown in Figure 1. From this Figure, we see that the stress – strain relation is given by Eq. (2)

$$\sigma = E(\epsilon_t - \epsilon_0) \qquad (2)$$

The strain energy per unit volume, u, is equal to the shaded area in Figure 1. And is given by $u = \frac{1}{2}\sigma\ \varepsilon_t$, This flexural strain energy is due to total strain minus thermal strain, Eq. (3).

$$u = \frac{1}{2}(\epsilon_t - \epsilon_0)E(\epsilon_t - \epsilon_0) \qquad (3)$$

The total strain energy *U* in the structure is obtained by integrating u over the volume of the structure of length L and cross sectional area A, given by Eq. (4)

$$U = \int_L \frac{1}{2}(\epsilon_t - \epsilon_0)E(\epsilon_t - \epsilon_0)\, A\mathrm{d}x \qquad (4)$$

3.2 Carbon Dependent Co-efficient of Linear Expansion:

The linear coefficient of thermal expansion, α, is dependent on atomic Carbon percentage [9] is given by $\alpha = (14.9\text{-}1.9C_m)*10^{-6}$ /^oC. Figure 2 shows for increase in Carbon percentage, there will be a decrease in linear expansion coefficient for Martensite steels. This variation is taken into consideration in the calculation of distortions and linear stresses which are evaluated for each of the four alloys considered. The objective of the study is to see the distortions and residual stresses caused by the temperature load due to the welding heat load θ. In Eq. (14) the finite element model of all the loads are obtained$\sum_e (\boldsymbol{f^e + T^e + \theta e + Pi})$. The flexural body loads f, surface loads T, and point loads P, cause elastic distortions and stresses which disappear on removal of these loads. However, the temperature induced distortions and stresses are permanent and remain same. Therefore, in Eq. 19 the net external force F is only due to temperature θ, thermal load.

In Table 1. Four AISI grades of Martensite steels are shown for evaluation. Apart from the element percentage composition, Atomic Number of each is given. Atomic weight and its percentage Atomic Weight is given. Atomic weight of Carbon is required for calculating the alloy linear coefficient of thermal expansion. It is seen that for AISI 4130 & AISI 4140 the Atomic Carbon percentage is 3.316%, for AISI4340 due to the presence of Ni, the carbon percentage atomic weight is less, 2.853 and for AISI4330 it is high, 4.356, due to the absence of S and Ph. Calculate percentage of Atomic weight of Carbon using following formula:

$$\text{Atomic weight \% of Carbon} = \frac{\frac{\text{Weight \% Carbon}}{Atomic\ \ weig\ ht\ of\ Carbon}}{\sum \text{of all elements of alloy}, \frac{\text{Weight \% element}}{Atomic\ \ weig\ ht\ of\ element}} * 100$$

Table1: Composition of Martensitic Stainless Steel

	Element	Cr	Mn	C	Si	Mo	S	Ph	Ni	Fe	Total
AISI#	Atomic Wt.	51.90	54.94	12.01	28.09	95.90	32.60	30.97	58.71	55.80	As reqd.
4130	Wt % Comp.	0.95	0.50	0.31	0.23	0.20	0.04	0.04	0.00	97.75	100.0
	Wt%/At. Wt	0.02	0.01	0.03	0.01	0.00	0.00	0.00	0.00	1.75	1.82
	At%C			1.40							
4140	Wt % Comp.	0.95	0.75	0.41	0.23	0.20	0.04	0.04	0.00	97.40	100.0
	Wt%/At. Wt	0.02	0.01	0.03	0.01	0.00	0.00	0.00	0.00	1.75	1.82
	At%C			1.85							
4330	Wt % Comp.	0.50	0.90	0.25	0.70	0.40	0.00	0.00	1.25	96.00	100.0
	Wt%/At. Wt	0.01	0.02	0.02	0.02	0.00	0.00	0.00	0.02	1.72	1.82
	At%C			1.15							
4340	Wt % Comp.	0.80	0.70	0.40	0.23	0.25	0.04	0.04	1.83	95.73	100.0
	Wt%/At. Wt	0.02	0.01	0.03	0.01	0.00	0.00	0.00	0.03	1.72	1.82
	At%C			1.83							

Based on the carbon atomic weight %, C_m, variation in linear coefficient of thermal expansion is calculated with a linear decrease is as C_m increases. In Figure 2, For AISI4330, $\alpha = 0.127*10^{-4}$; AISI4130, $\alpha = 0.122*10^{-4}$; AISI4340, $\alpha = 0.114*10^{-4}$; AISI4140, $\alpha = 0.113*10^{-4}$ The relation between α and C_m is linear and is decreasing with increasing C_m, atomic %, as seen in Figure 2. These values of α are used in the thermal load equation, $Q=\alpha\Delta T$.

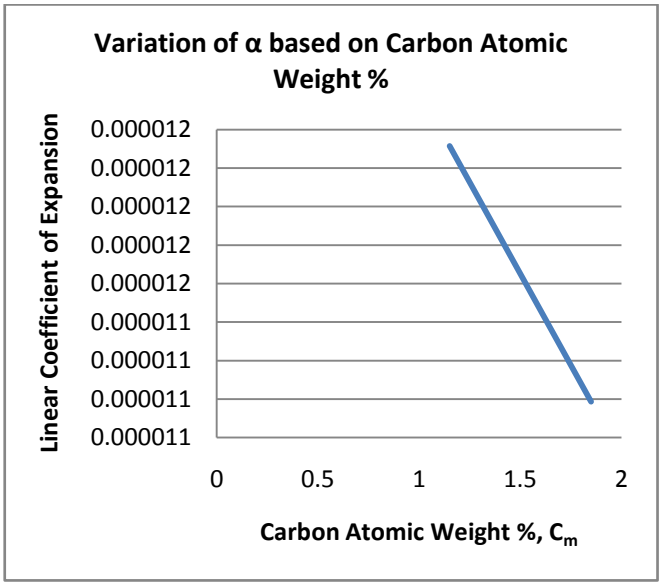

Figure 2: Variation of α, with Carbon Atomic Weight %

4. EXAMPLE OF BUTT WELDED JOINT

A Martenstic material of size 150mm length, 75mm width and 5 mm thick is welded with a similar material with 150mm along the length, 75mm lateral length on either side with a bead thickness of 5mm. This problem is symmetric in terms of thermal load, mechanical clamping, material, geometric & boundary conditions.

Length l=75mm, For Marten site material with Conductivity K=46W/m^{o}C, Convective heat transfer coefficient h=10W/m^{2o}C. The molten temperature is about 1460^{o}C. Boundary conditions are applied using the elimination approach which is more suiTable for hand calculations. The temperature distribution at fusion zone is at 1600^{o}C.

For structural problem, the load is differential temperature and coefficient of thermal expansion. Differential temperature from ambient of 25^{o}C is obtained from the thermal calculation. In this first step of thermal, finite element analysis of temperature distributions are obtained for two Boundary Conditions of specified temperatures and for specified heat at the fusion zone. In this Study the second case of specified heat at fusion and the resulting temperatures is taken for further structural distortions and residual stress analysis.

4.1 First Step: Heat of welding is input and Temperature distribution is output

Heat Flow problem is a scalar field problem with temperature T, as the field is variable. Though temperature is a scalar rate of heat flow or temperature change is a vector and it can have different values. Welding process having heat power in Watts, Q, is given through an Electric path, Q= ηVI, Where η is the process efficiency, V is the Volts and I is the current. This data is taken from [10].

From this equation Assuming K= $H_T + K_T$, the equation of steady state heat flux, W/m^2, is given by, after assembly, the linear simultaneous equations:

$T_e = K^{-1}\{R\}$

The solution is obtained after applying the boundary conditions and solving by any method like, Gaussian elimination method [1]. Among the temperature distributions evaluated, the selected one is having heat flux at the fusion zone of weld as shown in Figure (3). The temperature distribution is linearly decreasing from 1600^{o}to 30^o at the other end.

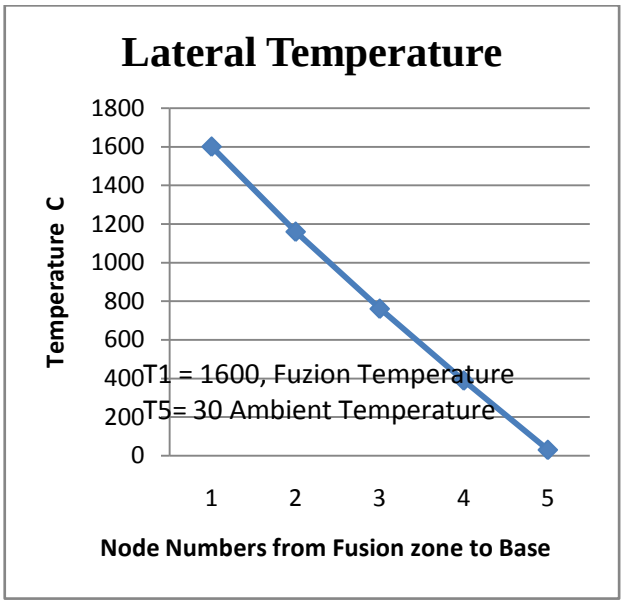

Figure 3: Welding Temperature for ambient temperature end

4.2 2nd Step: With the temperature obtained get thermal Load and calculate structural distortion and residual stresses.

The Natural coordinate, ξ, system used, is related to the Cartesian coordinates x, Eq. (5). Natural co-ordinate limits are -1 to +1 over the element length: $x_2 - x_1 = l_e$

$$\xi = \frac{2}{x_2 - x_1}(x - x_1) - 1 \qquad (5)$$

The derivatives in natural and Cartesian are also related, Eq. (6).

$$d\xi = \frac{2}{x_2 - x_1} dx = \frac{2}{le} dx \qquad (6)$$

In this equation l_e is the length of a 2 nodded 1D element. The Finite elements were given as combinations of the linear shape functions, N1 & N2. From Figure 4 the displacement, $q(\xi)$, at any point, $\xi, -1 < \xi < 1$. in the element is given in terms of nodal displacements and shape functions Eq. (7).

$$q(\xi) = N_1 q_1 + N_2 q_2 \qquad (7)$$

$= Nq^e$, Vector N gives temperature within element in terms of the nodal displacements, q^e

Where, N is a vector of shape functions and q^e is vector of nodal variables q_1 and q_2. The derivatives give the strain, $(\epsilon_t - \epsilon_0) = \frac{dq}{dx}$, given in Eq. (8) :

$$\frac{dq}{dx} = \frac{dq}{d\xi}\frac{d\xi}{dx}$$

$$= \frac{2}{\text{le}}\frac{dN}{d\xi} \cdot q^e$$

$$= \frac{1}{\text{le}}[1, \quad 1]q^e$$

$$\frac{dq}{dx} = B_T q^e \qquad (8)$$

Where, $B_T = \frac{1}{\text{le}}[-1, \quad 1]$ (9)

Vector B_T gives strain variation in the element in terms of the nodal displacements.

$\xi = -1)$ $2(\xi = +1)$

Figure 4. A Linear Element with thermal Load.

A linear Finite element in 1D is shown in Figure - 3 using a natural co-ordinate system in ξ. For a structure modeled with linear elements, along with Eq. (9) total strain energy is in Eq. (10)

$$U = \sum_e \frac{1}{2} A_e \frac{l_e}{2} \int_{-1}^{1} (\epsilon - \epsilon_0)^T E_e (\epsilon - \epsilon_0) d\xi \quad (10)$$

Noting that $\epsilon = Bq$, we get summation of element, e, matrices for the structure. The total potential energy, $\prod$ is given in Eq. (11).

$$\prod = \sum_e \frac{1}{2} q^T \left(E_e A_e \frac{l_e}{2} \int_{-1}^{1} B^T B d\xi \right) q - \sum_e q^T E_e A_e \frac{l_e}{2} \epsilon_0 \int_{-1}^{1} B^T d\xi + \sum_e \frac{1}{2} E_e A_e \frac{l_e}{2} \varepsilon_0^2 \quad (11)$$

investigative the strain energy expression, Rayleigh Ritz method of minimization of total potential energy with respect to the nodal displacements we get the equations of stiffness and load. The third term in Eq. (11) is a constant term and is of no consequence since it drops out of the equilibrium equations during derivative evaluation, which are obtained by setting d$\prod$ / dq =0.

The first term, $\left(E_e A_e \frac{l_e}{2} \int_{-1}^{1} B^T B d\xi \right)$, yields the element stiffness matrix, Eq. (12),

$$K_e = \frac{E_e A_e}{l_e} \begin{bmatrix} 1 & -1 \\ -1 & 1 \end{bmatrix} \quad (12)$$

The second term yields the desired element load vector θ^e, as a result of the temperature change:

$$\theta^e = E_e A_e \frac{l_e}{2} \epsilon_0 \int_{-1}^{1} B^T d\xi \quad (13)$$

From Equation 13 we can calculate θ^e for each of the elements and nodes. As we can see except for the relative load has positive and negative values are taken from Table 2 and added to get the net load. For these calculations, E will vary with the grade of the Marten site. The Coefficient of Linear expansion varies and is taken from the Table 1 as it varies with Martensite material grade and the Atomic percentage of Carbon in the material. The values of nodal temperature are from reference [10]. The first cell of first row gives temperature is at fusion, temperature drops to the end of the lateral surface to 30 ^{0}C. The second row is the ambient temperature and the third row gives the differential temperature. The last row gives the element temperature which is taken as the average of the two nodal temperatures.

Table 2. Temperature, ^{0}C distribution of element and nodes

Temp. node	1600	1160	760.6	410	30
T0	25	25	25	25	25
ΔT	1575	1135	735.6	385	5
Temp. element	1355	935.3	560.3	195	-

4.3 Definition of Problem: This model is adopted from the reference [10], a steady state heat transfer problem with no transient temperature, $\frac{dT}{dt}$, terms. The model has symmetry of heat input about the Fusion Zone. Symmetry is in geometry, material composition, heat input. Heat input is in the Fusion zone, which is at node 1, Figure 5. One part is considered lateral to the weld path. Node 1 has the high melting temperature due to heat load Q, say T(1) =1600^{o}C and the other end is insulated or heat flux q(n) =0, which is equal to an insulated end.

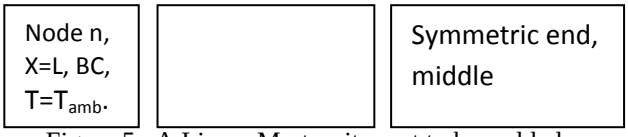

Figure 5. A Linear Martensite part to be welded

At X=0, heat is a thermal Load which causes a temperature change say along x, θ(x) a function of the distance x. For a Welding problem Heat flux, Q_e, is on the narrow region, represented by an element, as

directed by the electric arc, VIη. Figure 5, is a linear thermo- structural element with thermal load. Let A_e, be the cross sectional area, l_e, be the length of the element. The product $A_e l_e$ gives the volume of the element. We can have different Boundary Conditions, BCs of Structure, at end node, n: Clamped, Simply supported etc. There are two parts, the first part is a heat load. The output is a temperature distribution, t. The second part is a structural problem, with the temperature distribution as input load and with the structural BC which gives distortions and residual stresses. Doing these two problems sequentially is called a decoupled model, which is used in this study.

5. RESULTS

The 1D finite element simulation model is done in MS Excel. Two boundary conditions are considered. The welded material and process is considered symmetric thus, only one of the welded parts is considered for modeling. Instead of giving the load and getting melting temperatures, at node1, the Fusion Zone, FZ a temperature of melting 1600^{o}C is specified. The other end is considered as thermally insulated or q=0, no heat flows out from that end.

In Table2. The Nodal temperatures are obtained from the thermal analysis from reference [10]. Also the ambient temperature, T0, was 25 Degrees C. The net temperature, ΔT at each node, is the difference ΔT at each of the 5 nodes of the 4 elements in the system. The Temperature of each element is obtained by an average of the two nodes of the element, shown in Table 2.

In Table 3, the thermal Load For each element in the 4 element part to be welded is shown, the welding is to a similar part which is symmetric, hence, one of the parts is analyzed. Thermal Load, of element e is given by θe =A^e EαΔT. As shown in Table 3, the values are calculated as per Equation 13 Individual values are given in this Table, added values in Table 4.

Table 3. Nodal Thermal load at each node

Element ΔT/ Material	1355	935.3	560.3	195	E*10^9	α
AISI 4330	3871913	2672620	1601057	557212.5	2.4E+11	0.0000127
AISI 4130	2789606	1925549	1153518	401456.3	1.8E+11	0.0000122
AISI 4340	2027419	1399443	838348.9	291768.8	1.4E+11	0.0000114
AISI 4140	2870906	1981667	1187136	413156.3	2E+11	0.0000113

This equation can be simplified by substituting for B = $[-1 \quad 1]/(x_2 - x_1)$ and noting that $\epsilon_0 = \alpha\, \Delta T$. Thus Thermal load is given by Eq. (13)

$$\theta^e = \frac{E_e A_e l_e \alpha\, \Delta T}{x_2 - x_1} \begin{Bmatrix} -1 \\ 1 \end{Bmatrix} = E\, A_e \alpha\, \Delta T \begin{Bmatrix} -1 \\ 1 \end{Bmatrix} \qquad (13)$$

In Eq. 13, ΔT is the average change in temperature within the element. Table 4. Thermal load on the 5 nodes of each grade

Table 4: Nodal Thermal Load Added

Node load/ Material	**θ5**	**θ4**	**θ3**	**θ2**	**θ1**
AISI4330	-3871913	1199293	1071563	1043845	557212.5
AISI4130	-2789606	864057.4	772031.3	752061.4	401456.3
AISI4340	-2027419	627976.1	561093.8	546580.1	291768.8
AISI4140	-2870906	889239.4	794531.3	773979.4	413156.3

The temperature load vector can be assembled along with the body force, and point load vectors to yield the global load vector **F**, for the structure.

In Table 4. The Thermal load at every node is calculated at the Fusion node 1 from element 1 the load, θ1, say positive at that node from the other part to be butt welded also contributes because of the symmetric boundary condition, only one half is taken. As we move to the next node 2, the thermal load on the node is from element 1 is negative and from element 2 is positive the net load is θ2. Same process is continued until node 5 where there is no neighbouring node and only one element contributes to the thermal load. This process is from the thermal load of an element given in Equation 13, which has a positive value on one node and negative at the other.

Table 5: Element thermal load for each grade of material

Element stress	**σ=αΔTE**			
AISI4330	4130.04	2850.794	1707.794	594.36
AISI4130	2975.58	2053.919	1230.419	428.22
AISI4340	2162.58	1492.739	894.2388	311.22
AISI4140	3062.3	2113.778	1266.278	440.7

From the nodal thermal loads as in Table 5, we can calculate thermal stresses using equation σ=αΔTE. This may be obtained by dividing Elemental Thermal Load of Table 4 by the area of the element. The stresses in Fusion region are shown first and the last column gives the stress in the base material at the open end of the lateral surface. Among the Materials, AISI 4349 has the least stress and AISI 4330 the maximum. This stress variation is proportional to the Elastic modulus.

Apart from thermal load there can be other loads as given in Equation 14, including body forces $\boldsymbol{f^e}$, tractional forces $\boldsymbol{T^e}$, and point forces at nodes Pi. In this problem we have considered only Thermal Load. This assembly can be denoted as

$$F = \sum_e (\boldsymbol{f^e} + \boldsymbol{T^e} + \boldsymbol{\theta^e}) + \boldsymbol{Pi} \qquad (14)$$

For a Linear Element body force, f, in the element is distributed to nodes $\boldsymbol{f^e}$, given by Eq. (15)

$$f^e = \frac{l_e A_e f}{2}\begin{Bmatrix}1\\1\end{Bmatrix} \qquad (15)$$

Similarly, the traction force, T, in the element is distributed to nodes $\boldsymbol{T^e}$, given by Eq. (16). These temperatures are obtained from Thermal stiffness matrix, [10], from k_T, the

$$P^e = \frac{Pi}{2}\begin{Bmatrix}1\\1\end{Bmatrix} \qquad (16)$$

5.1 Structural Problem:

Once the temperature is obtained and total load vector F of combined thermal and structural is obtained, then we apply Rayleigh Ritz method of minimizing the total potential energy to obtain the equations of equilibrium of forces.

The above equations give the total potential energy, ∏, as Eq. (17)

$$\prod = \frac{1}{2}\mathrm{qT}Kq - \mathrm{qT\ F} \qquad (17)$$

Applying Rayleigh Ritz method of variation of total Potential energy, ∏, with respect to each of the nodal displacements, q, we get the equations of equilibrium of forces Eq. (18)

$$\mathbf{Kq} = \mathbf{F} \qquad (18)$$

The element stiffness matrix given as $\frac{E_e A_e}{l_e}\begin{bmatrix}1 & -1\\-1 & 1\end{bmatrix}$ where A_e is the element cross sectional area, E_e, is the element Young's Modulus; l_e is the element length l_e. Assembly of the elemental stiffness matrices using the common node compatibility condition gives the global or structural stiffness matrix K. Once the global stiffness matrix and force vector are obtained the global nodal wise displacement vector, q, is obtained by solving Equation 18 by applying the structural boundary conditions by elimination method. Table 6 gives the stiffness matrix in

Table 6: Unconstrained Stiffness Matrix

1200	-1200	0	0	0
-1200	2400	-1200		0
0	-1200	2400	-1200	0
0	0	-1200	2400	-1200
0	0	0	-1200	1200

The stiffness matrix of the structure, K, Table 6, obtained by assembling the element stiffness matrix given as $\frac{E_e A_e}{l_e}\begin{bmatrix} 1 & -1 \\ -1 & 1 \end{bmatrix}$ where A_e is the element cross sectional area, E_e, is the element Young's Modulus, A_e is the element cross sectional area and Element length l_e. Equation 18 is solved for displacements, q, by applying the structural boundary conditions by elimination or penalty method.

From Displacements, relative motions give distortions and also we can get residual stresses due to the flexural load and thermal load as below.

$$\sigma_e = E_e(\boldsymbol{Bq} - \alpha\, \Delta \boldsymbol{T}) \qquad (19)$$

$$\sigma_e = \frac{E_e}{\text{le}}[-1 \quad 1]q_e - E_e \alpha_e\, \Delta T_e \qquad (20)$$

In Eq. (19) or (20), is the combined structural and thermal stress is shown. These two are separately calculated. The thermal stresses are shown in Figures 6 & 7. Structural stresses in Table 7.

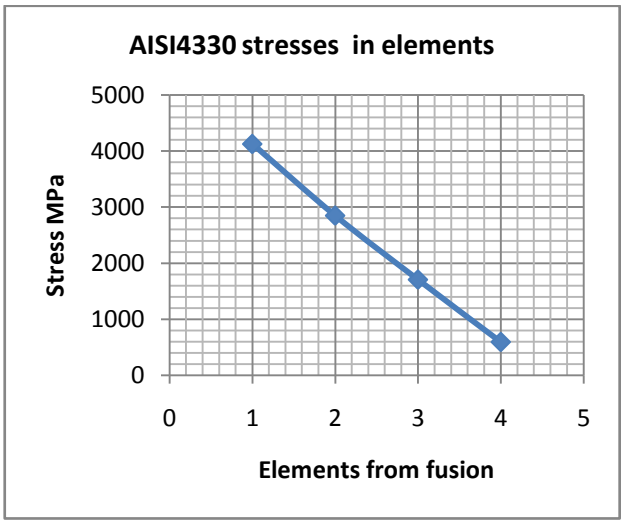

Figure 6: Thermal stress in AISI4330

The thermal stresses vary from the fusion region of node 1 to the least in the base material at the free end as shown in Figure 6. for AISI4330 material.

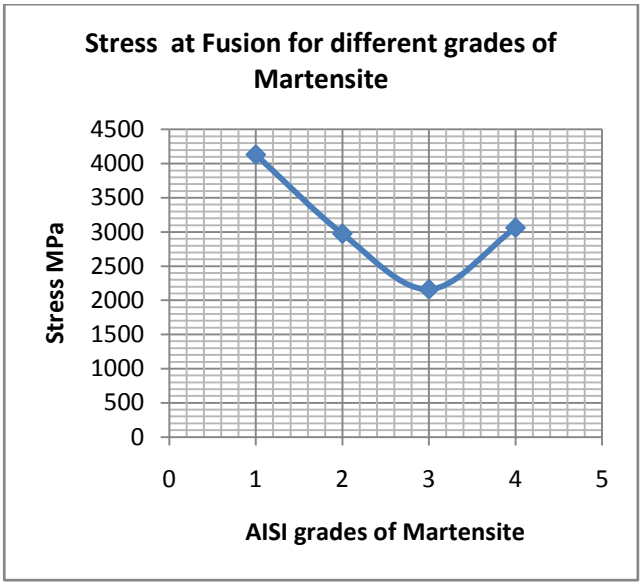

Figure 7. Thermal stresses for Martensite grades of steel

The structural displacement obtained with the base material end is fixed and it is obtained by solving Equation 20. An elimination approach is used to obtain the displacements of nodes stating at fusion end node 1 to fixed node 5.

Table7: Structural stress

Node	q, mm	element σ
1	7.252	20.925
2	6.787	58.68
3	5.483	101.565
4	3.226	145.17
5	0	

From the nodal displacements obtained the structural Stress in each element can be obtained as σ= E(q2-q1)/L as shown in Table 7 for AISI 4330 material. It might be observed that the structural stresses are far less by about 30 times than the thermal stresses. Hence the formation of residual stresses due to the thermal loading on the material is due to welding.

6. CONCLUSION

A One Dimensional Heat Transfer model was made using Finite Element Method to evaluate the distortions and stresses due to the thermal load in four grades of Martensite steels using 1D FEM.

- The Carbon Atomic % affect on the coefficient of linear expansion α, is evaluated for each of the grades. The Atomic % of C is inversely proportional to α. α is least for AISI4140 and Highest for AISI4330, .0000127.
- Thermal temperatures are proportional to the temperature distribution highest for AISI4330 and lowest for AISI4340.
- The net thermal load varies from negative value to positive value; for AISI4330 it changes from -3871913N to 1199293N
- Thermal stresses are maximum at Fusion 4130N/m^2 compared to 594.4 N/m^2 at the base material end. It may be observed that at fusion as melting and reformation happens yield stress comparison reoccurs after the weld solidifies.
- Thermal stresses are maximum for AISI4330 and least for AISI4340 for a similar welding process; reason is that these stresses are proportional to the modulus of elasticity.
- Structural stresses are far less, about 30 times, than the thermal stresses and hence the residual stresses are due to the thermal loads of welding.

  Welding stresses for four grades of Marten site steels are calculated using MS-Excel and can be formulated with far more generality in Mat lab.

REFERENCES

[1] Bathe, K. J., Finite Elements in Engineering, PHI, Delhi-110092, 2014.

[2] Thirupathi R Chandraputla, Ashok D Belegundu, Introduction to Finite Elements in Engineering, PHI, DELHI-110092, 2014.

[3] Reddy, J. N., Energy and Variational Methods in Applied Mechanics with An Introduction to the Finite Eement Method, New York: Wiley – Interscience, 1984

[4] Effect of Heat Flow Condition in Analysis of Electron Beam Welding, Suresh Akella, HarinadhVemanaboina, Ramesh Kumar Buddu, Sreyas IJST., Volume(1) –Issue(1), 2016,pp1-9, DOI:123.2016011001

[5] Heat Flux for Welding Processes: Model for Laser Weld, Suresh Akella; HarinadhVemanaboina, Ramesh Kumar Buddu, Sreyas IJST., Volume(1) –Issue(1), 2016,pp1-9, DOI:123.2016011002.

[6] An Analysis of Mechanical Behavior of AISI4130 Steel after TIG and Laser Welding Process, F Souza Neto, et al, Procedia Engineering 114 (2015) 181-188.

[7] A Comparative Evaluation of Microstructural and Mechanical behavior of fiber Laser Beam and Tungsten Inert Gas dissimilar Ultra High Strength Steel Welds, Jaiteerth R Joshi, et al, Defence Technology 12(2016)464-472.

[8] D. A. Porter and K. E. Easterling, Phase Transformations in metals and alloys, Chapman & Hall, 1992, p. 172 ISBN 0-412-45030-5.

[9] EJ Pagounis, E. Haimi, et al., Effect of thermal expansion coefficients on the Martensitic transformation in a steel matrix composite , Scripta Materialia, Vol. 34, No. 3, pp. 407-413,1996 Elsevier Science Ltd.

[10] D V Paleshwar, et al, Finite element formulation of welding process: Simulation of Martensitic steels, Sreyas International Journal of Scientists and technocrats, Vol. 2 (3) 2018, PP5-12.